

经颞下和乙状窦前入路显露岩尖部的虚拟现实解剖学研究

汤可 周敬安 周青 赵亚群 刘策

【摘要】 目的 在虚拟现实解剖模型中量化比较经颞下入路与经乙状窦前入路显露岩尖部的显微解剖学特征。方法 利用 15 例(30 侧)尸头 CT 和 MRI 影像构建岩尖部虚拟现实三维解剖模型。在颅盖上分别选取颞骨颧突根部上缘和乳突尖部为经颞下和乙状窦前入路的开颅标记点, 颅底上选择岩尖部为显露标记点, 以开颅和显露标记点连线为轴线作圆柱模拟经颞下和乙状窦前入路手术路径, 观察和测量两种手术路径中解剖结构显露情况, 采用配对 *t* 检验进行比较分析。结果 经颞下入路手术路径经过颅中窝底和颞叶到达岩尖部, 磨开岩骨后显露内耳道、面神经和迷路, 向前显露三叉神经、岩上窦和海绵窦。经乙状窦前入路经乳突磨除岩骨, 经面神经垂直段向深部依次显露颈静脉球、后组脑神经、听骨链、迷路和颈内动脉, 路径到达内耳道时显露小脑前下动脉和面听神经复合体, 到达岩尖部时包含小脑上动脉、岩上窦、岩下窦、海绵窦、三叉神经和部分颞叶。经乙状窦前入路手术路径中骨性结构、面听神经复合体、迷路和静脉体积均大于经颞下入路($P=0.000$), 颞叶、三叉神经和听骨链体积均小于经颞下入路($P=0.000$)。经乙状窦前入路中包含后组脑神经体积为(32.38 ± 2.86) mm^3 、包含颅底动脉体积为(262.74 ± 16.93) mm^3 , 经颞下入路不包含上述结构。结论 经乙状窦前入路对岩骨周围和岩骨内结构的显露范围多于经颞下入路, 对重要结构保护较好; 经颞下入路经过颞叶到达岩尖部, 适用于治疗累及岩骨并将颞叶向上推挤的颅中窝病变。

【关键词】 颞骨岩部; 神经解剖学; 显微外科手术

Comparison of subtemporal versus presigmoidal approaches for exposing petrous apex utilizing virtual reality technique

TANG Ke, ZHOU Jing-an, ZHOU Qing, ZHAO Ya-qun, LIU Ce

Department of Neurosurgery, the 309th Hospital of Chinese PLA, Beijing 100091, China

Corresponding author: TANG Ke (Email: tkshoushuda@sina.com)

【Abstract】 **Objective** To perform quantitative comparison of microanatomical features between subtemporal and presigmoidal minimally invasive approaches for exposing petrous apex on the basis of virtual reality image model. **Methods** CT and MRI were performed on 15 adult cadaver heads (30 sides) to establish virtual reality three-dimensional anatomical model of petrous apex. The superior edge of the root of temporal bone zygomatic process and the mastoidale on the calvaria were selected as landmark points of craniotomy through subtemporal and presigmoidal approaches. Petrous apex was selected as exposure landmark point on the skull base. The lines between craniotomy and exposure landmark points were used as axis to outline a cylinder simulating surgical routes of subtemporal and presigmoidal approaches. Anatomical exposures in two surgical routes were observed and measured. Statistical comparison was launched by paired *t* test. **Results** Surgical route of subtemporal approach passed through middle skull base and temporal lobe, and then reached petrous apex. Petrous bone drilling was performed to expose internal acoustic meatus, facial nerve and labyrinth. Then, trigeminal nerve, superior petrous sinus and cavernous sinus were exposed. Surgical route of presigmoidal approach was performed by drilling petrous bone through mastoid and passing vertical segment of facial nerve. Then, glomus jugulare, the lower cranial nerves, ossicular chain, labyrinth and internal carotid artery (ICA) were exposed in turn.

doi:10.3969/j.issn.1672-6731.2016.07.008

基金项目: 首都卫生发展科研专项基金资助项目(项目编号: 首发 2014-4-5073)

作者单位: 100091 北京, 解放军第三〇九医院神经外科

通讯作者: 汤可 (Email: tkshoushuda@sina.com)

Reaching internal acoustic meatus, the route exposed anterior inferior cerebellar artery (AICA) and facial-acoustic nerve complex. Reaching petrous apex, the route involved superior cerebellar artery, superior petrous sinus, inferior petrous sinus, cavernous sinus, trigeminal nerve and partial temporal lobe. The volumes of route, osseous structures, facial-acoustic complex, labyrinth and vein involved in presigmoidal approach were more than those in subtemporal approach ($P = 0.000$, for all). Volumes of temporal lobe, trigeminal nerve and ossicular chain involved in subtemporal approach were more than those in presigmoidal approach ($P = 0.000$, for all). Volume of lower cranial nerve and artery involved in presigmoidal approach was $(32.38 \pm 2.86) \text{ mm}^3$ and $(262.74 \pm 16.93) \text{ mm}^3$ respectively, but above structures were not involved in subtemporal approach. **Conclusions** Exposure of structures in and around petrous bone in presigmoidal approach is more than that in subtemporal approach. Thus, more attention should be paid to protect critical structures in presigmoidal approach. Subtemporal approach can reach petrous apex through temporal lobe, thus it is suitable to treat lesions in middle skull base which implicate petrous bone and push temporal lobe upward.

【Key words】 Petrous bone; Neuroanatomy; Microsurgery

This study was supported by Capital Medical Science Development Foundation (No. 2014-4-5073).

岩尖部位于颅中窝和颅后窝交界处,毗邻大脑后动脉(PCA)、海绵窦、岩上窦、中脑、动眼神经、滑车神经、三叉神经和外展神经等重要结构,手术解剖十分复杂,一旦损伤神经血管,术后将出现严重并发症^[1]。经颞下入路行岩尖部肿瘤切除术,由颞区切开颅骨,经颅中窝底到达岩骨嵴和岩尖部^[2];而经乙状窦前入路行岩尖部肿瘤切除术则经乳突磨除岩骨,手术路径涉及岩骨内面神经垂直段、半规管、内淋巴囊等结构的显露与保护,向其深部可于乙状窦前方到达脑干腹侧和岩尖部^[3]。比较上述两种神经外科手术入路的解剖学显露特点,有助于选择合理手术路径,因此,笔者采用虚拟现实技术,模拟上述两种手术入路显露岩尖部的三维解剖场景,测量并比较手术路径中各种解剖结构的显露情况。

材料与方法

一、实验材料

1. 标本来源 15例(共30侧)成人尸头标本购自北京大学医学部解剖学实验室,死亡原因均为心肌梗死(2007年6月-2009年3月),男性11例,女性4例;年龄60~71岁,平均65.31岁。标本以体积分数为10%甲醛溶液固定,通过双侧颈总动脉(CCA)和椎动脉(VA)灌注混合碘海醇注射液的红色硫化胶,通过双侧颈内静脉灌注上述混合碘海醇注射液的蓝色硫化胶。

2. 实验仪器 通过CT和MRI扫描获得尸头DICOM格式影像数据,CT扫描采用日本TOSHIBA公司生产的Aquilion ONE 320层动态容积CT扫描仪,扫描参数:球管电压120 kV、球管电流300 mA,

扫描范围260 mm,旋转时间0.75 s,矩阵 512×512 ,窗宽300、窗位40,层厚0.50 mm、层间距0.50 mm。MRI扫描采用荷兰Philips公司生产的PHILIPS 1.5T MRI扫描仪,扫描参数:三维自旋回波序列(SE)-T₁WI,重复时间(TR)11.30 ms、回波时间(TE)4 ms,翻转角(FA)15°,扫描视野(FOV)为22 cm × 22 cm,矩阵 512×512 ,扫描层厚1 mm、层间距为零,扫描范围260 mm,扫描时间12 min。影像学数据采集方法和参数参见文献[4]。Vitreax虚拟现实系统由日本TOSHIBA公司提供。

二、实验方法

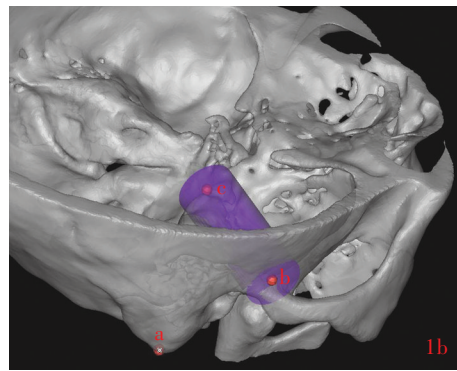
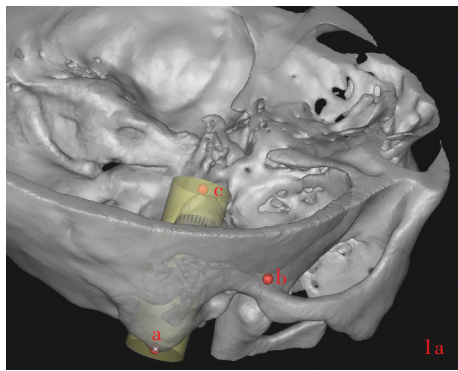
1. 模拟手术 采用DICOM格式影像数据,经光盘输入Vitreax虚拟现实工作站构建岩尖部周围结构三维解剖影像模型,方法参见文献[5]。分别选择颞骨颞突根部上缘作为经颞下入路手术切开颅骨之标记点、乳突尖部为经乙状窦前入路手术切开颅骨之标记点、岩尖部为颅底显露标记点;颅骨切开标记点与显露标记点之间连线形成轴线,制作直径为2 cm的圆柱模拟两种手术路径空间,观察该圆柱路径空间中所包含的解剖结构并测量其体积。

2. 统计分析方法 采用SPSS 16.0统计软件进行数据处理与分析,两种手术路径所获得的测量数据以均数±标准差($\bar{x} \pm s$)表示,采用配对 t 检验。以 $P \leq 0.05$ 为差异具有统计学意义。

结 果

一、手术路径解剖显露

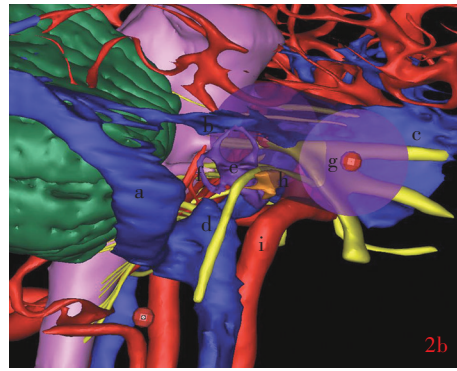
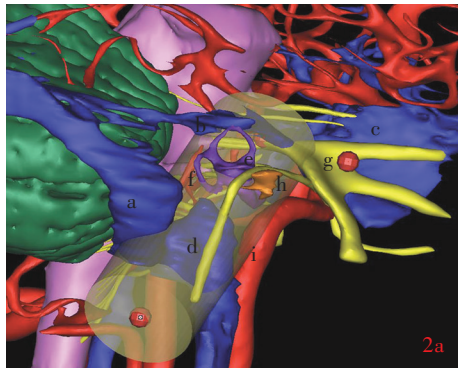
1. 经颞下入路 由颞骨鳞部进入,经颅中窝底到达岩尖部(图1),路径所涉及的颞叶解剖结构包



a, mastoidale, 乳突尖部; b, the superior edge of the root of temporal bone zygomatic process, 颞骨颧突根部上缘; c, petrous apex, 岩尖部

图1 手术路径与骨性结构之间的关系 1a 经乙状窦前入路手术路径(黄色圆柱) 1b 经颞下入路手术路径(紫色圆柱)

Figure 1 Relationship between surgical routes and osseous structures. Surgical route of presigmoidal approach (yellow cylinder, Panel 1a). Surgical route of subtemporal approach (purple cylinder, Panel 1b).



a, sigmoid sinus, 乙状窦; b, superior petrous sinus, 岩上窦; c, cavernous sinus, 海绵窦; d, vertical segment of facial nerve, 面神经垂直段; e, labyrinth, 迷路; f, facial-acoustic nerve complex, 面听神经复合体; g, trigeminal nerve, 三叉神经; h, ossicular chain, 听骨链; i, internal carotid artery, 颈内动脉

图2 手术路径与神经和血管之间的关系 2a 经乙状窦前入路手术路径(黄色圆柱) 2b 经颞下入路手术路径(紫色圆柱)

Figure 2 Relationship between surgical routes and neurovascular structures. Surgical route of presigmoidal approach (yellow cylinder, Panel 2a). Surgical route of subtemporal approach (purple cylinder, Panel 2b).

括颞下回前部、枕颞外侧回前部、枕颞内侧回前部和海马旁回前部;到达岩尖部前磨开岩骨显露内耳道和部分前庭、耳蜗,内耳道内可显露面神经,以及经膝状神经节向后外侧走行的面神经、膝状神经节和岩浅大神经。路径向前内侧可显露脑池段三叉神经前部和半月神经节后部,显露的静脉结构包括岩上窦内侧和海绵窦后部(图2)。

2. 乙状窦前入路 由乳突开始,向内侧于乙状窦前方磨除岩骨(图1),路径中包含部分乙状窦前缘,经面神经垂直段向深部显露部分颈静脉球顶部和后组脑神经,进而到达颈内动脉(ICA)岩骨段背侧部分及听骨链、部分后半规管、前庭和耳蜗;到达内耳道时,可显露部分小脑前下动脉(AICA),以及

脑池段和内耳道段的前庭上神经、前庭下神经、耳蜗神经和面神经;磨除岩骨到达岩尖部时,显露部分小脑上动脉(SCA)、岩上窦内侧部分、岩下窦上部、海绵窦后部、三叉神经脑池段和半月神经节后方腹侧部。路径中显露的幕上结构包含位于颞叶底部内侧的部分海马旁回前部(图2)。上述两种路径与骨性结构的关系见图1,与神经和血管的关系见图2。

二、两种手术入路各项参数的比较

于三维影像模型分别测量两种手术路径、路径中骨性结构(不包含听骨链)、面听神经复合体、迷路和静脉体积,结果显示,经乙状窦前入路路径中上述结构体积大于经颞下入路且差异有统计学意

表 1 经颞下入路与经乙状窦前入路显露岩尖部各项解剖学数据的比较($\bar{x} \pm s, \text{mm}^3$)**Table 1.** Comparison of anatomical data through subtemporal approach versus presigmoidal approach for exposing petrous apex ($\bar{x} \pm s, \text{mm}^3$)

Measurement item	Subtemporal approach (N = 30)	Presigmoidal approach (N = 30)	t value	P value
Volume of surgical path	14 859.00 ± 647.92	18 449.00 ± 682.16	-19.945	0.000
Volume of bony structure	4 663.90 ± 217.32	9 573.90 ± 262.53	-85.893	0.000
Volume of temporal lobe	5 830.10 ± 193.63	552.82 ± 27.89	149.248	0.000
Volume of facial-acoustic nerve complex	51.41 ± 2.70	145.35 ± 18.24	-27.612	0.000
Volume of trigeminal nerve	221.49 ± 19.54	135.30 ± 15.50	18.099	0.000
Volume of labyrinth	65.85 ± 3.33	224.17 ± 23.28	-37.713	0.000
Volume of vein	316.32 ± 22.43	1 900.30 ± 177.02	-48.900	0.000
Volume of ossicular chain	17.56 ± 3.27	0.47 ± 0.18	28.794	0.000

义(均 $P = 0.000$);而经乙状窦前入路路径中颞叶、三叉神经和听骨链体积则小于经颞下入路且差异有统计学意义(均 $P = 0.000$,表 1)。经乙状窦前入路所包含的后组脑神经体积为 $(32.38 \pm 2.86) \text{mm}^3$ 、颅底动脉体积 $(262.74 \pm 16.93) \text{mm}^3$,而经颞下入路不涉及上述解剖结构。

讨 论

在我们以往利用虚拟现实技术进行颅底解剖建模和测量的过程中,已勾勒出不同方向和大小的手术路径^[6],通过测量路径中解剖结构体积以评价创伤和显露范围,为神经外科手术提供量化证据并论证手术路径之适应证,以期建立手术相关三维影像数据指导体系^[7]。这一研究过程充分体现出现实技术高效、节约、个体化、精确化、量化之优势^[8]。在神经外科处理位于小脑幕切迹下方、脑干前方、半月神经节等部位的病变时,如岩斜区脑膜瘤和听神经瘤等,涉及对岩尖部的操作,经颞下入路和经乙状窦前入路均可到达岩尖部,如何选择合理的入路成为颅底手术解剖研究的重要任务。因此在本研究中,我们在虚拟现实建模条件下,通过呈现直观量化的证据对两种手术入路显露岩尖部的解剖学特征进行比较。

在我们以往的研究中,设计的圆柱手术路径体积能够反映手术器械之活动范围^[9],当两种圆柱底面直径一致时,路径体积即反映器械的操作深度。以显露岩尖部为主的手术,经乙状窦前入路的路径体积大于经颞下入路,考虑是由于乳突到岩尖部的

距离较远,而颞骨颞突根部上缘到岩尖部的距离较近,故形成体积差异。骨性结构体积则反映遮挡和磨除骨性结构操作的费时程度^[10],经乙状窦前入路手术需磨除的骨性结构体积大于经颞下入路。因此,经乙状窦前入路磨除岩骨的操作较经颞下入路更为费时。当经乙状窦前入路磨除岩骨形成操作路径后,可以避免对小脑半球的牵拉,到达岩尖部时需抬起部分颞叶组织,该部分颞叶组织所占体积较小;而经颞下入路对颞叶的牵拉和抬起范围较大,术中对脑组织的损伤程度高于经乙状窦前入路手术。

当手术路径到达岩尖部时,路径前端包含的解剖结构体积即提示手术入路对目标区域的显露程度^[11]。其中磨开内耳道时,经乙状窦前入路在后外下方向前内上方显露面听神经复合体,而经颞下入路则由前外上方向后内下方显露面听神经复合体,前者显露体积明显多于后者,考虑前者手术路径主要位于岩骨内,更邻近内耳道,因此对内耳道及其周围组织结构的显露具有一定优势。在显露面听神经复合体的过程中,两种手术入路均经听骨链和迷路,不同的是经乙状窦前入路包含迷路多于经颞下入路,而经颞下入路包含听骨链多于经乙状窦前入路,无论迷路还是听骨链的损伤都可使听力丧失^[12],因此,当病变由岩尖部向内耳道方向侵犯时,若累及听骨链较多时以选择经颞下入路手术为宜,而病变累及迷路较多时选择经乙状窦前入路手术更佳。手术路径前端显露三叉神经时,经颞下入路显露体积多于经乙状窦前入路,同时由于经颞下入路朝后内下方显露,三叉神经位于面听神经复合体前上方^[13],故在其手术路径中面听神经复合体未对三叉神经形成遮挡,而经乙状窦前入路朝前内上方显露,则路径中对三叉神经的显露受面听神经复合体的遮挡,因此,经颞下入路较经乙状窦前入路更适用于显露位于岩尖部的三叉神经。路径前端包含的静脉为岩上窦和后海绵窦相连接部以及邻近岩尖的三叉神经,因此,经颞下入路显露静脉体积也大于经乙状窦前入路。

本研究通过虚拟现实技术构建的手术路径,主要通过限定路径方向和范围前提下探讨解剖显露和创伤情况,其优点为可产生量化的指导数据^[4],但手术路径本身较为机械,与真实手术操作诸如组

织牵拉等情况存在较大差异^[14]。随着计算机导航和手术操作联合技术的不断进步,真实手术路径有望愈加接近术前模拟手术路径,对手术路径的比较将结合实际手术操作进一步得到验证。由于本研究样本量较小,关于解剖变异对手术路径比较结果的影响尚待扩大样本量进一步研究。

参 考 文 献

[1] Iacoangeli M, Salvinelli F, Di Rienzo A, Gladi M, Alvaro L, Greco F, Carassiti M, Scerrati M. Microsurgical endoscopy - assisted presigmoid retrolabyrinthine approach as a minimally invasive surgical option for the treatment of medium to large vestibular schwannomas. *Acta Neurochir (Wien)*, 2013, 155:663-670.

[2] Tang K, Li Y, Zhou JA, Zhou Q, Liu C, Zhao YQ. Simulation of petrous bone drilling in subtemporal approach utilizing virtual reality system. *Zhongguo Xian Dai Shen Jing Ji Bing Za Zhi*, 2012, 12:736-740.[汤可, 李阳, 周敬安, 周青, 刘策, 赵亚群. 经颞下入路磨除岩骨虚拟现实模拟研究. *中国现代神经疾病杂志*, 2012, 12:736-740.]

[3] Tang K, Zhou Q, Zhou JA, Zhao YQ, Liu C. Minimally invasive research of presigmoidal approach for exposure of jugular foramen region utilizing virtual reality system. *Zhongguo Xian Dai Shen Jing Ji Bing Za Zhi*, 2015, 15:311-315.[汤可, 周青, 周敬安, 赵亚群, 刘策. 虚拟现实系统对乙状窦前入路微创显露颈静脉孔区的解剖学研究. *中国现代神经疾病杂志*, 2015, 15:311-315.]

[4] Tang K, Bao SD, Zhou JA, Zhou Q, Liu C, Zhao YQ. Quantitative research of microsurgical anatomy of transfrontal approach for cavernous sinus by virtual reality skill. *Zhongguo Xian Dai Shen Jing Ji Bing Za Zhi*, 2011, 11:590-594.[汤可, 鲍圣德, 周敬安, 周青, 刘策, 赵亚群. 虚拟现实技术量化经额入路显露海绵窦区显微解剖研究. *中国现代神经疾病杂志*, 2011, 11:590-594.]

[5] Tang K, Zhou JA, Zhou Q, Zhao YQ, Liu C. Anatomic research of suboccipito - retrosigmoidal approach for minimally invasive exposure of facial - acoustic nerve complex utilizing virtual reality skill. *Zhongguo Xian Dai Shen Jing Ji Bing Za Zhi*, 2014, 14:502-506.[汤可, 周敬安, 周青, 赵亚群, 刘策. 枕下乙状窦后入路微创显露面听神经复合体的虚拟现实解剖研究. *中国现代神经疾病杂志*, 2014, 14:502-506.]

[6] Tang K, Zhou JA, Zhou Q, Liu C, Zhao YQ. Exposing cavernous sinus through transfrontal vs transorbital approach: a quantitative comparison with virtual reality system. *Di San Jun Yi Da Xue Xue Bao*, 2013, 35:145-148.[汤可, 周敬安, 周青, 刘策, 赵亚群. 联合入路中经额与经眶颧方向显露海绵窦手术的虚拟现实量化比较. *第三军医大学学报*, 2013, 35:145-148.]

[7] Tang K, Yuan XD, Zhou JA, Zhou Q, Zhao YQ, Liu C. Research of minimally invasive design for suboccipito - retrosigmoidal approach to expose jugular foramen region by virtual reality skill. *Shen Jing Ji Bing Yu Jing Shen Wei Sheng*, 2014, 14:137-139.[汤可, 袁小东, 周敬安, 周青, 赵亚群, 刘

策. 枕下乙状窦后入路显露颈静脉孔区微创策略的虚拟现实研究. *神经疾病与精神卫生*, 2014, 14:137-139.]

[8] Zhou Q, Tang K, Zhou JA, Yuan XD. Application of virtual reality combined with Flair imaging skills in three-dimensional anatomy of nucleus surrounding the lateral ventricle. *Zhonghua Shen Jing Yi Xue Za Zhi*, 2014, 13:69-72.[周青, 汤可, 周敬安, 袁小东. 虚拟现实结合 Flair 成像在侧脑室周围核团三维解剖研究中的应用. *中华神经医学杂志*, 2014, 13:69-72.]

[9] Tang K, Zhou JA, Zhao YQ, Zhou Q, Liu C. Anatomic research of suboccipito - retrosigmoidal approach for minimally invasive exposure of jugular foramen region utilizing virtual reality technology. *Di San Jun Yi Da Xue Xue Bao*, 2014, 36:1496-1499.[汤可, 周敬安, 赵亚群, 周青, 刘策. 枕下乙状窦后入路微创显露颈静脉孔区的虚拟现实解剖研究. *第三军医大学学报*, 2014, 36:1496-1499.]

[10] Xue XS, Ye XZ, Huang Y, Chen JY, Chu WH, Zou MM, Chen F, Lin JK. Clinical analysis of posterior lamina internal fixation for the treatment of atlantoaxial dislocation with craniovertebral junction region malformation. *Zhongguo Xian Dai Shen Jing Ji Bing Za Zhi*, 2012, 12:448-452.[薛兴森, 叶信珍, 黄毅, 陈景宇, 储卫华, 邹明明, 陈飞, 林江凯. 经后路椎板内固定术治疗颅颈交界区畸形合并寰枢椎脱位. *中国现代神经疾病杂志*, 2012, 12:448-452.]

[11] Fahmy CE, Carrau R, Kirsch C, Meeks D, de Lara D, Solares CA, Otto BA, Prevedello DM. Volumetric analysis of endoscopic and traditional surgical approaches to the infratemporal fossa. *Laryngoscope*, 2014, 124:1090-1096.

[12] Komatsu F, Komatsu M, Di Ieva A, Tschabitscher M. Endoscopic extradural subtemporal approach to lateral and central skull base: a cadaveric study. *World Neurosurg*, 2013, 80:591-597.

[13] Li HH, Yue SY, Li YG, Han JG, He ZZ. A microanatomical study on the surrounding structures of the cisternal segment of trigeminal nerve. *Zhongguo Xian Dai Shen Jing Ji Bing Za Zhi*, 2010, 10:662-667.[李海红, 岳树源, 李勇刚, 韩建国, 贺中正. 脑池段三叉神经周围结构的显微解剖. *中国现代神经疾病杂志*, 2010, 10:662-667.]

[14] Tang K, Zhou JA, Zhao YQ, Zhou Q, Liu C. Surgical anatomy research of transcondyle approach for exposure of jugular tubercle utilizing virtual reality technique. *Shen Jing Ji Bing Yu Jing Shen Wei Sheng*, 2014, 14:552-554.[汤可, 周敬安, 赵亚群, 周青, 刘策. 经枕髁入路显露颈静脉结节的虚拟现实手术解剖研究. *神经疾病与精神卫生*, 2014, 14:552-554.]

(收稿日期:2016-05-03)

本期广告目次

欧来宁(石药集团欧意药业有限公司)	封二
醒脑静(江西济民可信医药有限公司)	对封三
和信(海南中和药业有限公司)	封三
申捷(齐鲁制药有限公司)	封四